

1 **Increased respiration by the oxidative pentose phosphate pathway in chloroplasts at high**
2 **atmospheric CO₂ concentration – Supporting information**

3 Thomas Wieloch

4

5 **Notes S1. Recalculation of previously reported estimates of flux through the plastidial**
6 **anaplerotic pathway at low C_a**

7 In Wieloch *et al.* (2022), we expressed fractionation signals discussed here as

8

$$\delta D_i = \frac{D_i}{\Sigma D_{ME}/6} - 1 \quad \text{Eqn S1}$$

9

10 where D_i and D_{ME} denote relative deuterium abundances of specific carbon-bound hydrogens
11 of glucose and the six methyl-group hydrogens of the glucose derivative used for NMR
12 measurements (3,6-anhydro-1,2-*O*-isopropylidene- α -D-glucofuranose), respectively. Here, I
13 express these signals as

14

$$\delta D_1 = \frac{D_1}{D_{6S}} - 1 \quad \text{Eqn S2}$$

15 and

16

$$\delta D_2 = \frac{D_2}{D_{6R}} - 1 \quad \text{Eqn S3}$$

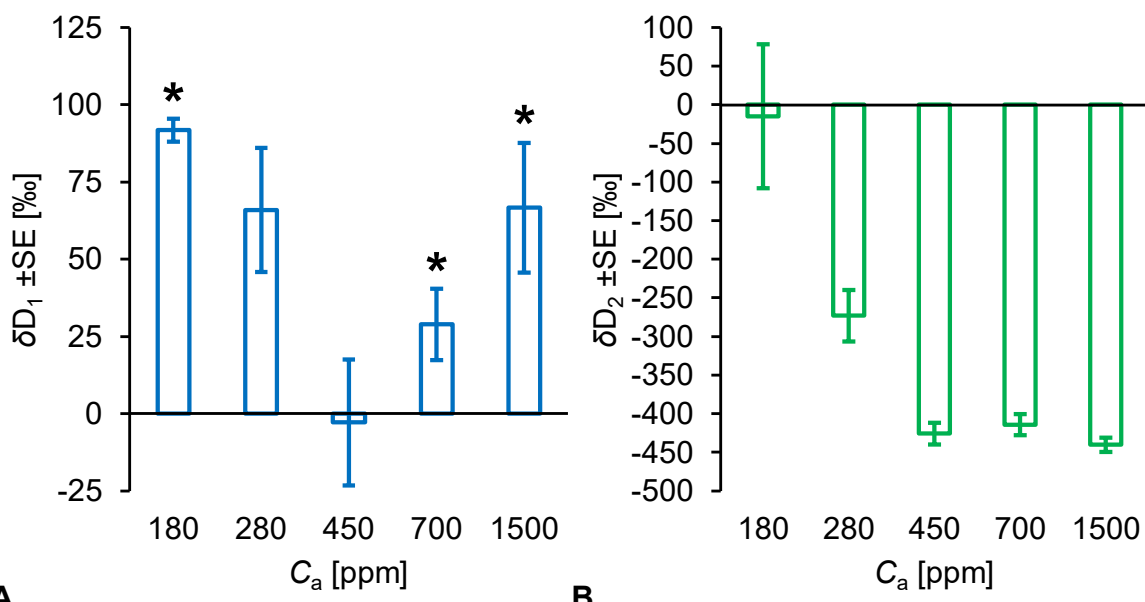
17

18 Based on equation S2, δD_1 is 66‰ at $C_a = 280$ ppm and 92‰ at $C_a = 180$ ppm (Figure S1A).
19 Furthermore, δD_1 and thus flux through the plastidial anaplerotic pathway is significantly
20 greater than zero at $C_a = 180$ ppm ($p < 0.05, n = 2$) while it comes close to being significantly
21 greater than zero at $C_a = 280$ ppm ($p < 0.13, n = 2$). A previously published model describing
22 deuterium fractionation by G6PD can be used to estimate the plastidial anaplerotic flux, and
23 associated respiration (Wieloch *et al.*, 2022). Based on this model, ≈ 9.3% and 12.7% of the
24 G6P entering the starch biosynthesis pathway is diverted into the anaplerotic pathway at $C_a =$
25 280 and 180 ppm, respectively. Assuming 50% of all net assimilated carbon becomes starch
26 (Sharkey *et al.*, 1985), anaplerotic flux and associated respiration proceeds at ≈ 5% and ≈ 7%
27 relative to the rate of net carbon assimilation at $C_a = 280$ and 180 ppm. These rates are probably
28

29 strongly underestimated since, at low C_a , much of the fractionation signal introduced by G6PD
30 can be expected to not arrive in starch (see biochemical explanation in Wieloch *et al.*, 2022).

31
32 Based on equation S3, δD_2 is $\approx -427\text{‰}$ at $C_a \geq 450$ ppm, -273‰ at $C_a = 280$ ppm, and -15‰ at
33 $C_a = 180$ ppm (Figure S1B). This indicates that the PGI reaction is on the side of F6P at $C_a \geq$
34 450 ppm and shifts towards equilibrium with decreasing C_a below 450 ppm (Wieloch *et al.*,
35 2022).

36



37
38 **Figure S1** Deuterium abundance at glucose H¹ (A, blue bars), and H² (B, green bars) of
39 sunflower leaf starch. Asterisks denote deuterium abundances that are significantly greater than
40 zero (one-tailed one-sample t-test: $p < 0.05$, $n \geq 2$). At 280 ppm, δD_1 is close to being
41 significantly greater than zero ($p < 0.13$, $n = 2$). The plants were raised in chambers over 7 to 8
42 weeks at $C_a = 450$ ppm. After a day in darkness to drain the starch reserves, the plants were
43 grown for two days at different levels of C_a (180, 280, 450, 700, 1500 ppm) corresponding to
44 different levels of C_i (140, 206, 328, 531, 1365 ppm). Data expressed as $\delta D_1 = D_1/D_{6S}-1$ and
45 $\delta D_2 = D_2/D_{6R}-1$ where D_i denotes relative deuterium abundances at specific carbon-bound
46 hydrogens of glucose. Deuterium abundances at glucose H^{6S} and H^{6R} are used as references
47 because glucose H¹ and H^{6S} and H² and H^{6R} have the same precursors at the chloroplast triose-
48 phosphate level, and H^{6S} and H^{6R} are not modified in the starch biosynthesis pathway (Wieloch
49 *et al.*, 2022).

50

51 **References**

52 **Sharkey TD, Berry JA, Raschke K. 1985.** Starch and sucrose synthesis in *Phaseolus vulgaris*
53 as affected by light, CO₂, and abscisic acid. *Plant Physiology* **77**: 617–620.

54 **Wieloch T, Augusti A, Schleucher J. 2022.** Anaplerotic flux into the Calvin-Benson cycle.
55 Hydrogen isotope evidence for *in vivo* occurrence in C₃ metabolism. *New Phytologist* **234**: 405–
56 411.

57